The EMBO Journal (2011) 30, 145–153 | © 2011 European Molecular Biology Organization | Some Rights Reserved 0261-4189/11
www.embojournal.org

THE EMBO JOURNAL

EMBO open

Replication termination and chromosome dimer resolution in the archaeon *Sulfolobus solfataricus*

Iain G Duggin[1,2,3,*], Nelly Dubarry[1] and Stephen D Bell[1,*]

[1]Sir William Dunn School of Pathology, Oxford University, Oxford, UK and [2]MRC Cancer Cell Unit, Hutchison/MRC Research Centre, Cambridge, UK

Archaea of the genus *Sulfolobus* have a single-circular chromosome with three replication origins. All three origins fire in every cell in every cell cycle. Thus, three pairs of replication forks converge and terminate in each replication cycle. Here, we report 2D gel analyses of the replication fork fusion zones located between origins. These indicate that replication termination involves stochastic fork collision. In bacteria, replication termination is linked to chromosome dimer resolution, a process that requires the XerC and D recombinases, FtsK and the chromosomal *dif* site. *Sulfolobus* encodes a single-Xer homologue and its deletion gave rise to cells with aberrant DNA contents and increased volumes. Identification of the chromosomal *dif* site that binds Xer *in vivo*, and biochemical characterization of Xer/*dif* recombination revealed that, in contrast to bacteria, *dif* is located outside the fork fusion zones. Therefore, it appears that replication termination and dimer resolution are temporally and spatially distinct processes in *Sulfolobus*.

The EMBO Journal (2011) **30,** 145–153. doi:10.1038/emboj.2010.301; Published online 26 November 2010
Subject Categories: cell cycle; genome stability and dynamics
Keywords: archaea; DNA replication; site-specific recombination; termination; Xer

Introduction

Archaea have attracted considerable attention because of the orthologous relationship of their information processing machineries to those of eukaryotes. However, archaea have a prokaryotic cell structure and, like many bacteria, they have circular chromosomes. Some archaea, such as *Pyrococcus* spp., have a bacterial-like mode of chromosome replication, with a single origin of replication that initiates bidirectional replication (Myllykallio *et al*, 2000). In contrast, *Sulfolobus* spp. have three bidirectional replication origins per chromosome (Lundgren *et al*, 2004; Robinson *et al*, 2004, 2007; Duggin *et al*, 2008a). All three origins are activated in each round of replication within a narrow temporal window (Duggin *et al*, 2008a), and marker frequency analyses (MFAs) have revealed that replication forks meet approximately mid-way between the origins whereupon replication fork fusion (termination) occurs (Lundgren *et al*, 2004; Duggin *et al*, 2008a). However, it is unknown whether there are specific replication fork arrest sites that restrict fork fusion to a 'terminus' region, as in bacteria (Duggin *et al*, 2008b), or whether fork fusion occurs at essentially random sites mid-way between the origins.

A consequence of chromosome circularity is that an odd number of crossover events occurring between sister chromosomes will generate a chromosome dimer—a covalent fusion of the two newly replicated chromosomes. Any dimer that forms must be resolved accurately into monomers so that each daughter cell inherits one complete chromosome. Bacteria have a specific locus, called *dif*, where a crossover catalysed by the Xer site-specific recombinases resolves any chromosome dimers to monomers (Sherratt, 2003). In *Escherichia coli*, XerCD-mediated recombination at *dif* requires FtsK, a DNA translocase that is anchored at the mid-cell nascent division site. FtsK reads short-sequence motifs in the genome that are polarized towards *dif* and specifically translocates DNA, bringing the two *dif* sites together at mid-cell for synapsis. FtsK then stimulates catalysis by XerD (Aussel *et al*, 2002).

The conserved location of *dif* in the terminus region ($\sim$180° from the origin of replication) in a broad range of bacteria and the role of FtsK likely reflect the manner in which chromosome replication and segregation are coupled in bacteria. Visible segregation of newly replicated marker loci occurs soon after their duplication (Toro and Shapiro, 2010). The late replication and segregation of *dif* therefore reduce the work required of FtsK to align the *dif* sites at mid-cell. The replication termination systems of bacteria that restrict termination to the region containing *dif* are therefore expected to optimize this aspect of chromosome segregation (Duggin *et al*, 2008b). Evidence supporting a link between termination of replication and dimer resolution came when Lemon *et al* (2001) deleted the *Bacillus subtilis* gene encoding the replication terminator protein (*rtp*) in combination with deletions of either *ripX* or *spoIIIE* (*B. subtilis* homologues of XerD and FtsK, respectively). This led to an elevated production of anucleate cells, indicative of failed chromosome segregation. In *E. coli*, deletion of the replication terminator protein, Tus, worsened the reduced fitness seen in FtsK

*Corresponding authors. IG Duggin, MRC Cancer Cell Unit, Hutchison/MRC Research Centre, Hills Road, Cambridge CB2 0XZ, UK. Tel.: +44 1223 402402; Fax: +44 1223 213556;
E-mail: iduggin@mrc-lmb.cam.ac.uk or SD Bell, Sir William Dunn School of Pathology, Oxford University, South Parks Road, Oxford OX1 3RE, UK. Tel.: +44 186 527 5564; Fax: +44 186 527 5515;
E-mail: stephen.bell@path.ox.ac.uk
[3]Present address: MRC Laboratory of Molecular Biology, Hills Road, Cambridge CB2 0QH, UK

Received: 28 July 2010; accepted: 29 October 2010; published online: 26 November 2010

mutants defective in directional DNA translocation (Sivanathan *et al*, 2009).

In this study, we demonstrate that replication termination and chromosome dimer resolution are spatially distinct processes in the *Sulfolobus solfataricus* chromosome. The findings are congruent with a previous observation of an extended period of sister chromosome cohesion in *Sulfolobus* (Robinson *et al*, 2007), and suggest an explanation for how *Sulfolobus* cells can accommodate multiple active replication origins per chromosome.

Results and discussion

Analysis of replication intermediates in the fork fusion zones

We have previously described the use of neutral–neutral 2D gel electrophoresis to map replication termination events in the *E. coli* chromosome (Duggin and Bell, 2009). Similar approaches have been applied to map and characterize fork arrest sites in eukaryotic cells (Calzada *et al*, 2005). We performed a series of 2D gels to analyse overlapping restriction fragments covering the three general fork fusion zones previously identified from MFA. The resolution of the MFA performed by Lundgren *et al* (2004) accurately delimited replication origins to within 40 kb zones. Therefore, to search for termination sites, we analysed ~100 kb regions centred on the fork fusion zones between adjacent origins (oriC1/oriC2, oriC2/oriC3 and oriC3/oriC1). If defined termination sites exist, we would expect to detect a spot of greater intensity on the 'Y-arc,' corresponding to paused replication forks (Figure 1A). A spike of hybridization might also be detectable emanating from the pause spot, corresponding to replication forks approaching the paused fork from the other direction (Brewer and Fangman, 1988; Duggin and Bell, 2009). In contrast, if termination occurs at random positions along a given restriction fragment then these specific signals would not be detected and a diffuse cone-like feature might be detectable emerging from the replication fork arc, representing fork fusion at random positions along the fragment (Friedman and Brewer, 1995) (Figure 1A). As may be seen in Figure 1B–D, in many fragments we detected the faint cone signal, but we did not detect any specific replication pause sites in the ~320 kb that we analysed over the three fork fusion zones. We conclude that there is no evidence for site-specific termination within the fork fusion zones identified by MFA. Therefore, it appears that replication termination in *Sulfolobus* occurs by random collision of replication forks, as is believed to be generally the case in eukaryotes, rather than via a bacterial-like site-specific termination mechanism.

Phenotypes of xer-deleted cells

Replication termination, sister chromosome segregation and dimer resolution are interlinked processes in bacteria. It was therefore relevant to characterize the potential role of the Xer recombinase homologue. *S. solfataricus* has a single-Xer homologue, encoded by the SSO0375 open reading frame (She *et al*, 2001), that shares 31% amino acid sequence identity with *E. coli* XerD. We deleted the *xer* gene from the chromosome of strain PBL2025 by replacing it with the *lacS* marker using double-crossover homologous recombination, and confirmed the replacement using PCR and western blotting (Figure 2A). The resultant strain showed a growth-rate reduction compared with the parent strain PBL2025; co-culture revealed that this corresponded to a loss of fitness of 5.98% (±0.64) per generation when compared with the otherwise isogenic (but *lacS*-) strain, PBL2025 (Figure 2B). To investigate the possibility that the *lacS* marker had caused the growth defect in the Δ*xer::lacS* strain, we compared the Δ*flaJ::lacS* strain, which has a flagella defect (Szabó *et al*, 2007), with the parent PBL2025, and we observed no significant difference in growth rate (0.64% (±0.32) loss of fitness per generation; Figure 2B). Therefore, deletion of *xer* results in a loss of fitness.

To explore the possibility of cell division/cycle defects in the Δ*xer::lacS* strain, we began by measuring cell size in mid-log phase cell populations using a Coulter counter. As can be seen in Figure 2C, the Δ*xer::lacS* strain exhibited larger cell volumes compared to the parent PBL2025; the mean cell volumes were: PBL2025 = 0.720 (±0.001, s.e.m.) μm^3, compared to Δ*xer::lacS* = 0.866 (±0.001) μm^3. Furthermore, the Δ*xer::lacS* cell volume distribution had a greater skew towards cells of greater volume. For example, 8.2% PBL2025 cells were $>1\,\mu m^3$ versus 17.5% Δ*xer::lacS* cells, whereas 14.8% PBL2025 and 11.7% Δ*xer::lacS* cells were $<0.4\,\mu m^3$. This indicates a significant delay or failure of cell division in a subpopulation of cells in the Δ*xer::lacS* strain. These findings are highly reminiscent of the *E. coli dif* (deletion-induced filamentation) phenotype (Kuempel *et al*, 1991; Hendricks *et al*, 2000), and are consistent with a role for Xer in resolving chromosome dimers in *S. solfataricus*.

To examine chromosome segregation more directly, we measured the cellular DNA contents of mid-log phase cell populations by flow cytometry. PBL2025 had the characteristic distribution of *Sulfolobus* cells (Figure 2D, left panel), with 2N-content cells predominating due to the relatively long time these cells spend in the 2N (G2 + M) phases of the cell cycle. The Δ*xer::lacS* strain showed a significantly altered distribution of DNA content compared to PBL2025 (Figure 2D, right panel). In all, 26% of the Δ*xer::lacS* sample showed >2N genome equivalents, compared with 12% for PBL2025, and the DNA content of the >2N cells in the Δ*xer::lacS* sample was heterogeneous. Similar effects were observed after impairment of cell division of *S. solfataricus* (Samson *et al*, 2008). Δ*xer::lacS* also gave rise to an increased level of 'debris' or anucleate cells that have <1N genome equivalents of fluorescence with greater scatter signals (Figure 2D). Furthermore, the apparent 2N peak was significantly broader for the Δ*xer::lacS* strain, indicating DNA content heterogeneity. Microscopic examination of cells from the cultures examined by flow cytometry revealed clear differences between the strains that are consistent with the effects observed by flow cytometry (Figure 2E and F; Supplementary Figure S2). The Δ*xer::lacS* strain showed elevated frequencies of cells that were anucleate (or had very weak DAPI staining) and greater frequencies of cells that appeared to be undergoing chromosome segregation (Figure 2F). Rare dividing cells that had DAPI staining only on one side (Figure 2E, 'FS' label) were strongly suggestive of failed chromosome segregation, a likely cause of the generation of anucleate cells.

The above observations strongly suggest that Δ*xer::lacS* cells frequently encounter problems undergoing or attempting termination of replication or chromosome segregation. We conclude that the phenotypic characteristics of the

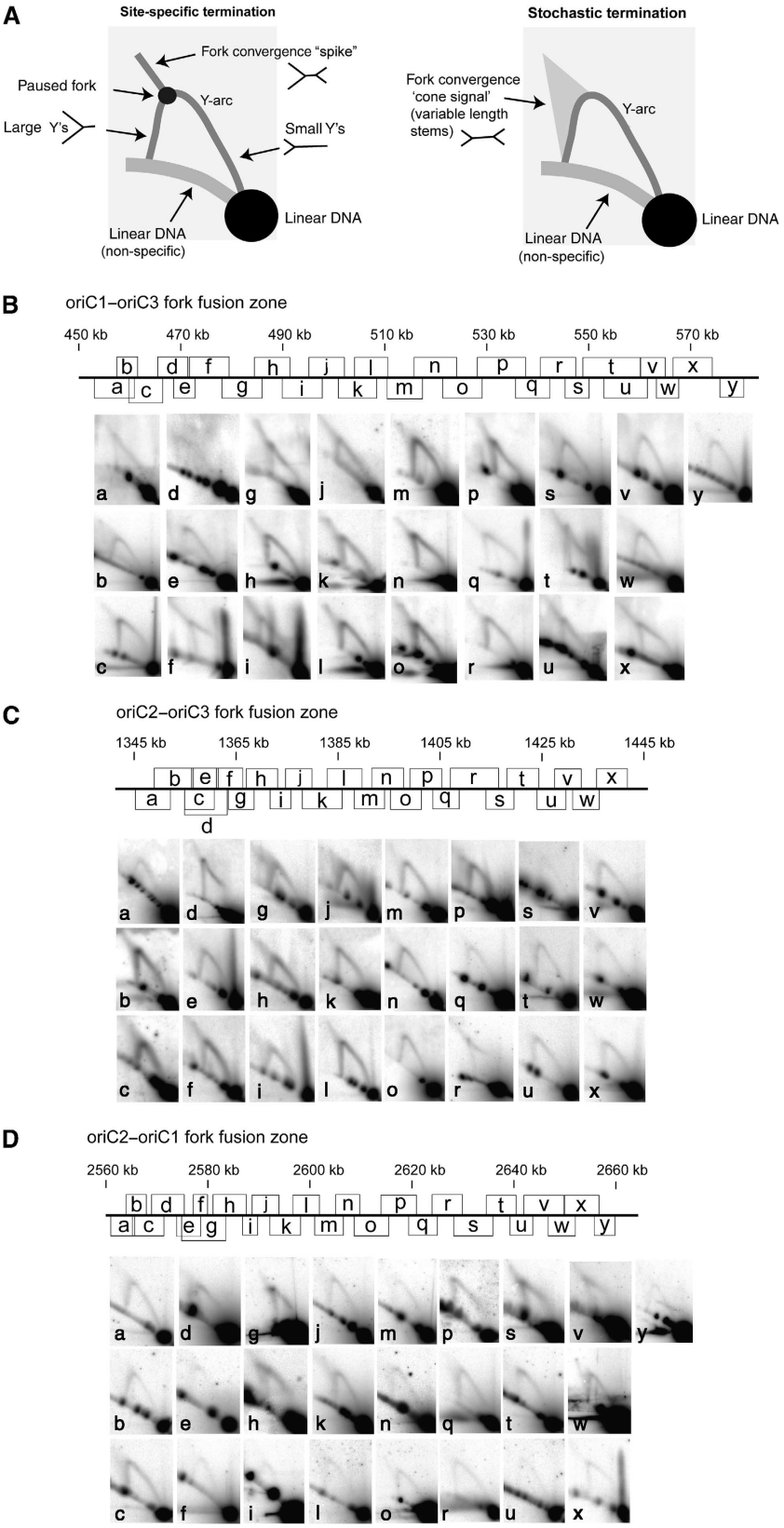

Figure 1 2D gel electrophoresis analysis of the fork fusion zones of *S. solfataricus* P2. (**A**) Cartoons depicting the possible outcomes of 2D gel analysis with respect to different mechanisms of replication termination. (**B**) oriC1–oriC3 fork fusion zone. (**C**) oriC2–oriC3 fork fusion zone. (**D**) oriC2–oriC1 fork fusion zone. The scale map in each panel indicates the genomic location of the restriction fragments and corresponding 2D gel results in the panels below. For each 2D gel, DNA from mid-log phase cells was digested with an appropriate restriction enzyme and then subjected to 2D agarose gel electrophoresis. The 2D pattern for each particular restriction fragment was then obtained by Southern hybridization. The coordinates for the fragments and probes are given in Supplementary Table S1, available at *The EMBO Journal* Online.

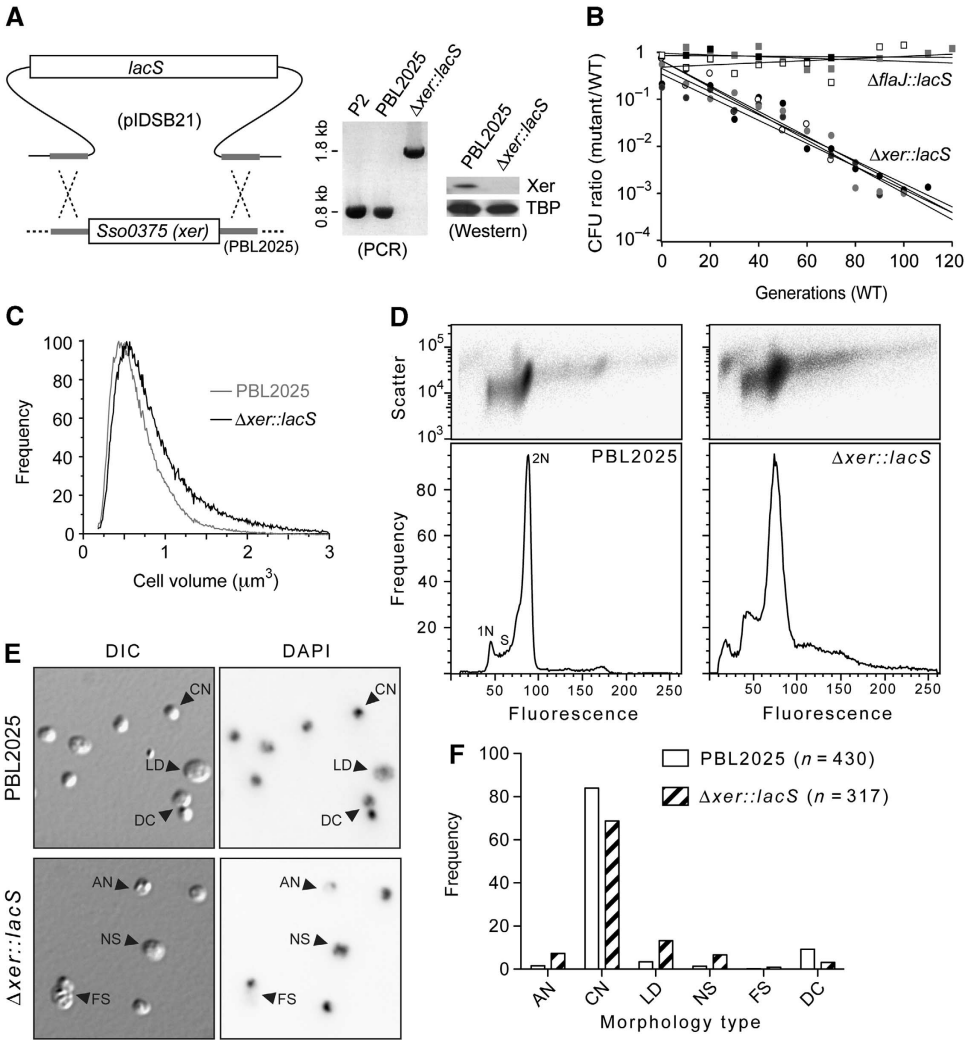

Figure 2 Deletion of *xer* and phenotypic effects on *S. solfataricus*. (**A**) Double-crossover recombination of linearized pIDSB21 with the PBL2025 chromosome results in the exchange of *lacS* for *xer*, which was confirmed by PCR using primers designed from the flanking regions, and western blotting using anti-Xer antibodies. The blots were then probed with anti-TATA box binding protein (TBP) as a loading control. (**B**) Growth competition between Δ*flaJ::lacS* (squares) or Δ*xer::lacS* (circles) and the parent PBL2025 (WT) strain. Results from three independent experiments for Δ*flaJ::lacS* versus PBL2025 and four independent experiments for Δ*xer::lacS* versus PBL2025 are shown. (**C**) Coulter cell volume analysis of mid-log phase PBL2025 and Δ*xer::lacS* populations. Data were normalized to their highest values. (**D**) Flow cytometry analysis of cellular DNA content for PBL2025 and Δ*xer::lacS*. Side-scatter 2D plots (upper panels) and fluorescence histograms (lower panels) are shown. (**E**) Representative light micrographs showing differential interference contrast (DIC) and fluorescence (DAPI) images acquired for the same field of cells from the indicated strains. Examples of the types of cells observed are indicated by arrowheads. AN, anucleate; CN, compact nucleoid; LD, large diffuse nucleoid; NS, nucleoid segregation; FS, failed segregation; DC, doublet or dividing cell. Further examples are provided in Supplementary Figure S2, available at *The EMBO Journal* Online. (**F**) Frequency analysis of the morphology types observed by microscopy. Each cell type was scored as percent of total cells.

Δ*xer::lacS* strain are consistent with a role for Xer in chromosome dimer resolution in *S. solfataricus*.

Identification of the S. solfataricus dif site

In bacteria, the Xer proteins act at a specific chromosomal site, *dif*, to bring about recombination and chromosome segregation. Although *dif* is conserved amongst bacterial species, searches of the *S. solfataricus* genome sequence with bacterial *dif* consensus sequences failed to clearly identify candidate sites. Furthermore, DNA sequence composition analyses, which have helped guide searches for *dif* sites previously, revealed only weak sequence compositional skew profiles that are inconclusive with regards to the location of *dif* (Zhang and Zhang, 2005). To identify a binding site(s) for Xer, we conducted an *in vivo* search of the *S. solfataricus* genome using a chromatin immunoprecipitation (ChIP)-based approach. DNA recovered from the Xer-ChIP was labelled and then used to interrogate microarrays that contained one oligonucleotide feature per open reading frame. The results of this 'ChIP-chip' approach, shown in Figure 3A, revealed significant enrichment of DNA hybridizing to probes for two adjacent open reading frames, SSO1161 and SSO1162, which are separated by a large intergenic region of ~650 nt. Having identified a candidate locus, the experiment was then repeated and ChIP recovered DNA was quantified by real-time PCR with locus-specific or distal control primers. The results, shown in Figure 3B, confirmed a highly significant enrichment for the 'dif2' and 'dif3' sequences in the intergenic SSO1161–SSO1162 region, indicative of a Xer-binding site(s) near these genes. Neither of these open reading

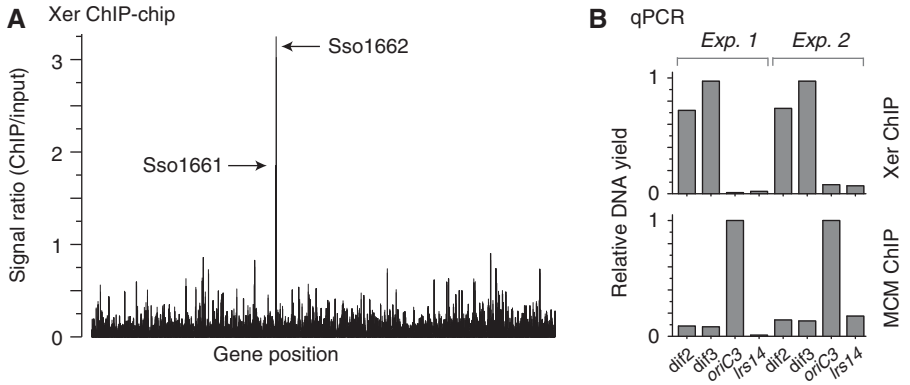

Figure 3 Identification of the Xer-binding '*dif*' locus in *S. solfataricus*. Xer was immunoprecipitated from formaldehyde-fixed and sonicated *S. solfataricus* P2 cell extracts, and bound DNA was analysed by the 'ChIP-chip' method and by quantitative real-time PCR. (**A**) ChIP-chip data for anti-Xer ChIP reactions, indicating the peak heights for ORFs SSO1161 and SSO1662, which show a significant enrichment above background. (**B**) qPCR analysis of anti-Xer and anti-MCM ChIP reactions, using the four indicated primer sets (dif2, dif3, *oriC3* and *lrs14*), in two sets of independent experiments. 'Input' DNA, purified from the cell extract used in the chromatin immunoprecipitations, was used to generate standard curves in quantification. Data were normalized to the highest yielding sample for each ChIP. The anti-MCM ChIP serves as a control reaction, in which MCM was expected to bind preferentially to origin DNA. The *lrs14* control locus was expected not to bind specifically to either MCM or Xer.

frames have an obvious connection to chromosome metabolism or cell division; SSO1161 encodes a protein of the higher eukaryote and prokaryote nucleotide-binding domain (HEPN) superfamily, SSO1162 encodes an efflux pump of the major facilitator superfamily.

To search for the specific binding site(s) for Xer within the SSO1161–1162 region, we first generated four overlapping PCR products from the intergenic region and used these in electrophoretic mobility-shift assays (EMSAs) using recombinant Xer. As shown in Figure 4A, the labelled fragment 'dif3', located approximately centrally in the intergenic region, exhibited two Xer-concentration-dependent mobility shifts, demonstrating specific binding by Xer to this fragment. Examination of the sequence of this fragment revealed three candidate dyad symmetric elements that we chose to analyse individually using EMSAs. Two of the dyad elements, named DYAD2 and DYAD3, overlap significantly (Figure 4B). We found that both sequences in isolation bound specifically to Xer (Figure 4B). However, DYAD2 only gave rise to one mobility-shifted species, whereas DYAD3 gave rise to two mobility-shifted species in a Xer-concentration-dependent manner, consistent with the previous EMSA in Figure 4A involving the much larger 'dif3' PCR fragment. These findings strongly suggest that DYAD3 is the *dif* site of *S. solfataricus*, with DYAD2 only sharing enough common sequence with DYAD3 to bind one subunit of Xer. Furthermore, DYAD3 shows recognizable sequence similarity to bacterial *dif* sites, including several of the most conserved bases that participate in sequence symmetry (Figure 4C). To test whether DYAD2 or DYAD3 acts as a *dif* site by acting as a substrate for Xer-mediated site-specific recombination, we next established a Xer-dependent recombination system.

The S. solfataricus dif site functions in intermolecular and intramolecular site-specific recombination

We inserted a series of double-stranded oligonucleotides with either wild-type or mutant DYAD2 and DYAD3 into pPCR-Script and assayed for plasmid multimerization *in vitro* in a Xer-dependent manner. We first tested a 50-bp DNA fragment encompassing both DYAD2 and DYAD3. As may be seen in Figure 5A, we observed a Xer-dependent multimerization of the plasmid, dependent on the presence of the 50-bp sequence containing DYAD2 and DYAD3 (compare 'empty vector' with 'dII–dIII', Figure 5A). Significantly, when we mutated DYAD2 but retained DYAD3 as wild type, we detected clear Xer-mediated recombination indistinguishable from the full-length wild-type sequence ('dII mutA' and 'dII mutB', Figure 5A). In contrast, the mutation of DYAD3 with preservation of DYAD2 abolished Xer-dependent recombination (Figure 5A, 'dIII mut'). Thus, in agreement with our conclusions from the EMSA experiments above, DYAD3 functions as a *dif* site in intermolecular recombination reactions containing purified Xer-6H.

Next, we inserted the *dif* site, either as the dif3 273nt PCR product or the isolated 38 bp DYAD3 sequence in tandem or inverted orientations in the plasmid, with a 1.8-kb fragment (containing *lacS*) between each site. Recombination between tandemly repeated sites would result in excision of the intervening DNA, whereas recombination between inversely oriented sites would invert the intervening DNA (Figure 5B, upper panels). As can be seen in the lower panel of Figure 5B, the 38-bp DYAD3 site was sufficient to generate the predicted intramolecular recombination products in both orientations. Therefore, the Xer-binding DYAD3 site that our *in vivo* and *in vitro* studies have identified acts as a *dif* site for Xer-mediated intramolecular and intermolecular recombination in a reconstituted system containing only the pure Xer protein. This contrasts with studies in *E. coli*, *Streptococcus pneumoniae* and *Vibrio cholerae*, where a complete recombination reaction at *dif* required the Xer recombinases and FtsK (Aussel *et al*, 2002; Val *et al*, 2008; Nolivos *et al*, 2010).

In bacteria, *dif* is located within the last-replicated region of the chromosome, $\sim 180^{\circ}$ across from the origin of replication. It is notable that in *S. solfataricus*, the *dif* site is located very asymmetrically between *oriC2* and *oriC3*. This inter-origin region is 1.27 Mbp in length with *dif* located 0.26 Mbp from oriC3 and 0.375 Mbp from the mid-point of the fork fusion zone (Figure 6). This organization strongly suggests that chromosome dimer resolution is spatially and temporally distinct from replication termination in *S. solfataricus*. Furthermore, the absence of FtsK homologues in *Sulfolobus* suggests that chromosome segregation and dimer resolution

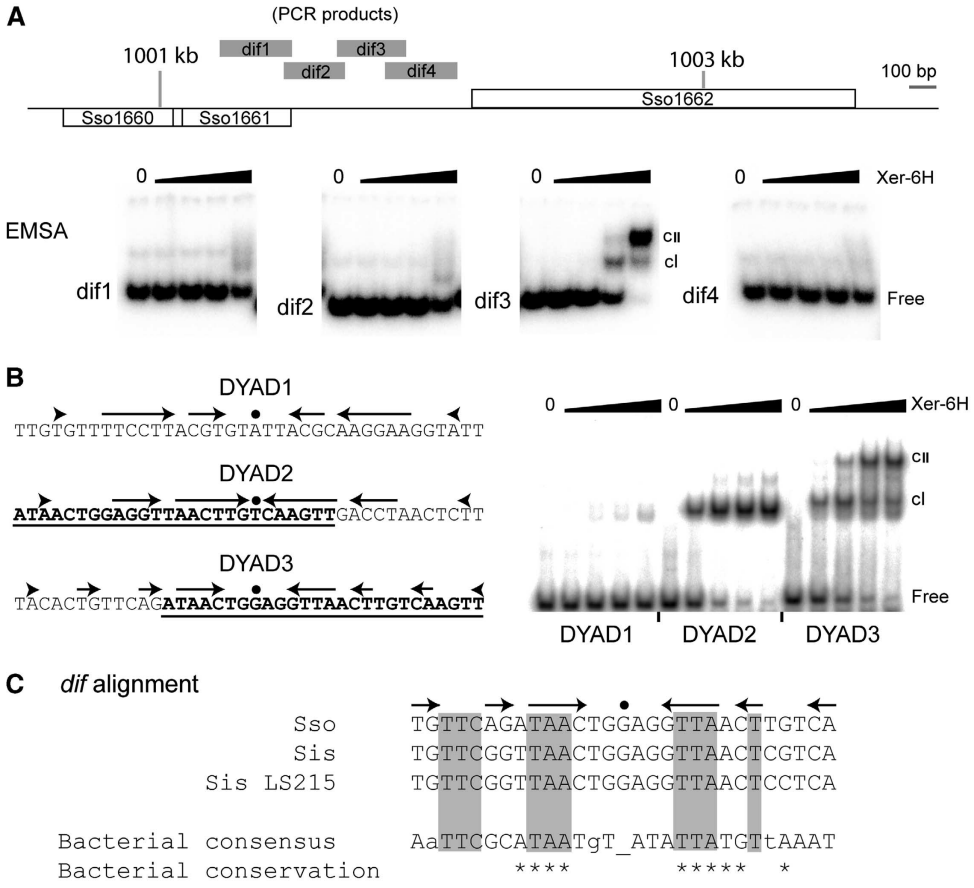

Figure 4 *In vitro* identification of the *dif* site. (**A**) EMSA analysis of the four PCR fragments indicated by grey bars in the map of the SSO1161–1162 region. Each reaction contained 5 nM labelled PCR product and 0, 8, 40, 200 or 1000 nM Xer-6H (by monomer, left to right, in each panel). (**B**) Sequences of the three dyads analysed from the dif3 PCR fragment. Arrows represent DNA sequence symmetry around the central dot. The underlined and bold sequences of DYAD2 and DYAD3 indicate their region of overlap. Double-stranded oligonucleotides of these sequences were end labelled and then used in EMSA reactions at 2 nM with 0, 19, 55, 167 or 500 nM Xer-6H, left to right in each case. cI and cII indicate the respective mobility-shifted complexes. (**C**) Alignment of the *dif* sequence (DYAD3) from *S. solfataricus* (Sso) with sites identified by similarity searching in closely related *Sulfolobus islandicus* (Sis; strain L.S.2.15 contains a single change compared with other sequenced strains), and the proteobacterial consensus sequence (Carnoy and Roten, 2009). Shading indicates sequence matching. Asterisks indicate positions with >90% conservation in proteobacteria, whereas positions with <50% conservation are shown as lower case letters.

are not linked in a bacterial-like manner. The relatively early replication of *dif* before termination in *S. solfataricus* suggests the existence of another mechanism to attain close proximity of *dif* sites until after replication termination. Previous data have suggested that *S. solfataricus* maintains its sister chromatids in a cohesed state for an extended period of time after replication (Robinson *et al*, 2007), and observations of chromosome conformation in whole cells suggested that segregation occurs relatively rapidly late in the cell cycle, well after termination of replication (Poplawski and Bernander, 1997). It is therefore possible that dimer resolution does not occur until an as-yet unidentified chromosome segregation machinery acts later in the cell cycle.

There is a considerable genetic load placed on bacterial chromosomes to ensure that dimer resolution at the *dif* site occurs at the appropriate time and place in the replication cycle. The sequence composition of the chromosome imparts directional cues to FtsK to ensure that DNA is pumped in the appropriate direction (Bigot *et al*, 2005, 2007; Lesterlin *et al*, 2008), and the *Ter* sites ensure that *dif* remains in the last replicating region of the chromosome (Duggin *et al*, 2008b). One consequence of having such highly tailored chromosomes is that if ectopic origins of replication integrate into the chromosome, they will likely result in an unsynchronized arrival of replication forks at termination sites and cause a premature replication and segregation of *dif*. This would consequently lead to inefficient prolonged stalling of replication forks and their potential collapse, and could result in failure to resolve chromosome dimers. The deleterious consequences of such scenarios are consistent with the observed maintenance of a single-replication origin per bacterial chromosome. In contrast, in *Sulfolobus*, we have found that termination occurs by stochastic collision of forks and the *dif* site is located well outside the fork fusion zones. These apparently less constrained features of the *Sulfolobus* genome structure may have imparted greater plasticity to replicon evolution in *Sulfolobus*, thus making ancestral *Sulfolobus* chromosomes receptive to additional origins of replication.

Materials and methods

Analysis of fork fusion zones by 2D gel electrophoresis

DNA from mid-log phase *S. solfataricus* P2 cells was extracted after embedding the cells in agarose plugs (Robinson *et al*, 2004). After digestion with each of the restriction enzymes indicated in Supplementary Table S1, 2D gel electrophoresis and Southern transfer were carried out as described (Duggin *et al*, 2008a). The

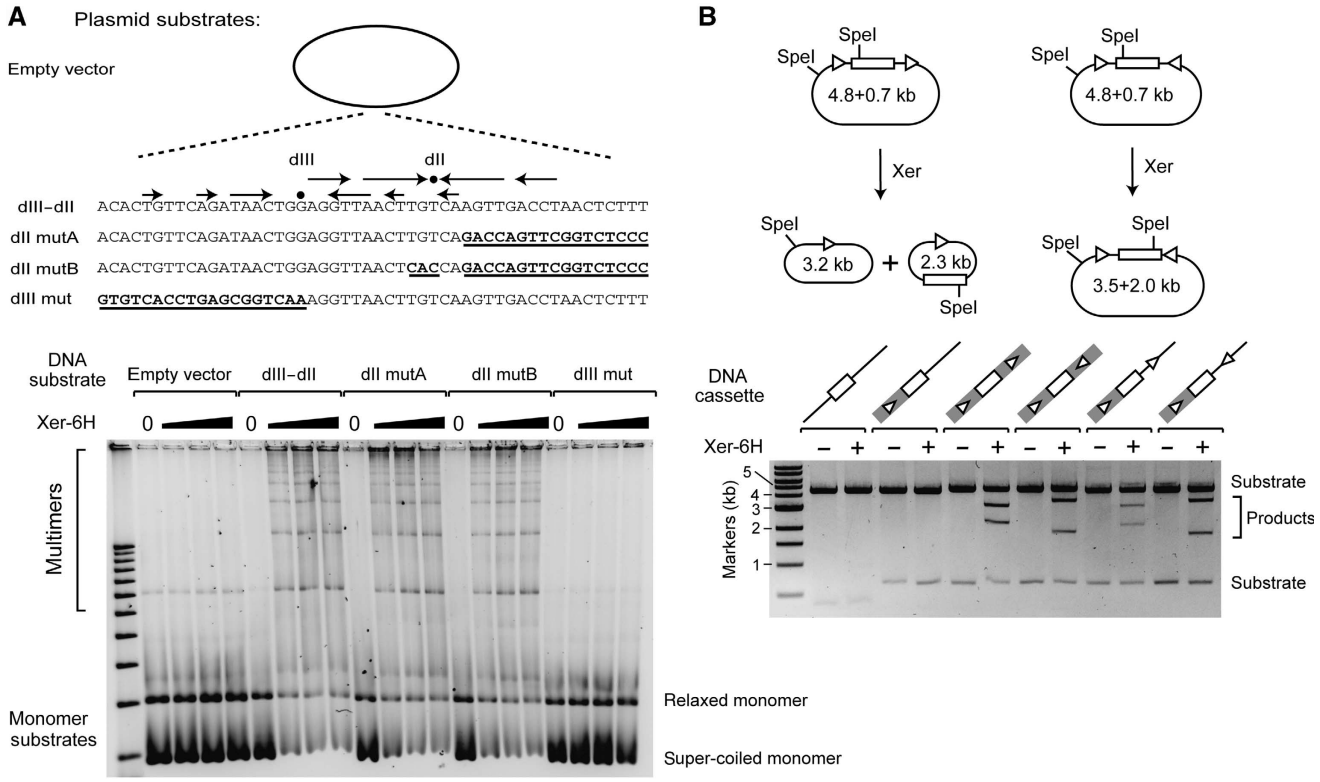

Figure 5 Xer is necessary and sufficient for recombination at *dif in vitro*. (**A**) Intermolecular recombination assays. Plasmids containing a 50-bp DNA fragment encompassing DYAD3 (dIII) and DYAD2 (dII), or a 50-bp DNA fragment mutated for dIII or dII (the mutated bases are represented by bold underlined text) were incubated with Xer-6H. Recombination products (plasmid multimers) were detected by agarose gel electrophoresis (lower panel). (**B**) Intramolecular recombination assays. (Upper panel) Plasmids containing two test sequences in either a direct or inverted repeat orientation flanking a *lacS* gene cassette were incubated with Xer-6H. After digestion by *Spe*I, the products were analysed by agarose gel electrophoresis. For each DNA substrate tested (lower panel), the 273-bp *dif3* PCR sequence is indicated by a grey box, whereas DYAD3, either in the context of the *dif3* PCR fragment (within the grey box) or cloned as a 38-bp double-stranded oligonucleotide, is indicated by a white triangle. The *lacS* gene is shown as a white box.

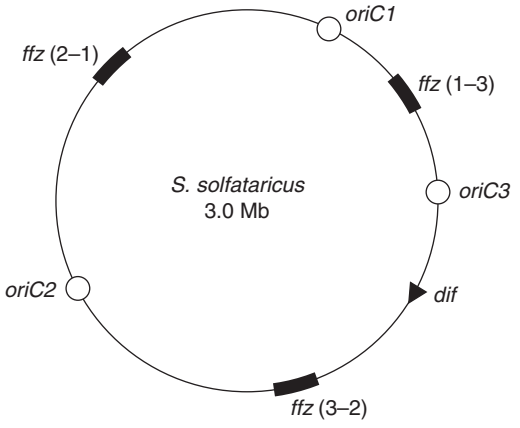

Figure 6 Overall replication organization of the *S. solfataricus* chromosome. Origins are indicated with open circles, the ~100-kb fork fusion zones [*ffz*(*x*–*y*), where *x* and *y* refer to adjacent origins] tested in Figure 1 are shown as thick black arcs and the *dif* site by a black triangle.

membranes were probed with ^{32}P-random-prime-labelled PCR products (~0.5 kb) that had been amplified from *S. solfataricus* P2 genomic DNA to target the appropriate restriction fragments (Supplementary Table S1, available at *The EMBO Journal* Online).

Xer-deletion strain construction and phenotypic analysis

The plasmid pIDSB21, for deletion of *xer* (Figure 2A), was constructed by sequentially cloning PCR products of the *xer* upstream (genome coordinates: 319885–319141) and downstream (318443–317686) flanking regions into the *Kpn*I–*Nco*I and *Bam*HI–*Not*I sites, respectively, of pET2268 (Szabó *et al*, 2007). pIDSB21 was linearized with *Kpn*I, purified, and then mixed with PBL2025 cells for electroporation as described (Albers and Driessen, 2008). Transformed cells were selected by liquid-culture growth for several passages in Brock's medium with 0.4% (w/v) lactose as the sole carbon source, followed by streak plating on Gelrite plates of the same media for isolation of clones. Double-crossover *xer*-deleted clones were identified by PCR, and western blotting using anti-Xer antisera.

For co-culture experiments, a 1:1 mixture of the two strains was grown in Brock's medium, containing tryptone (0.2%, w/v) and glucose (0.2%, w/v), at 75°C. Their relative frequencies were determined by plating every ~10 generations on Brock's tryptone/glucose (the permissive medium for WT and mutant strains) and on Brock's containing lactose 0.2% (w/v) (selective medium for the mutant strain). Data were analysed as described (Pérals *et al*, 2000).

Coulter cell volume analyses were carried out as described (Duggin *et al*, 2008a). For flow cytometry, cells were first fixed by mixing 0.3 ml of culture (A_{600} = 0.3) with 0.7 ml ice-cold ethanol and stored at 4°C. Cells were centrifuged for 5 min at 13 000 r.p.m. and resuspended in 1 ml 10 mM Tris–Cl (pH 7.4), 10 mM $MgCl_2$. Cells were centrifuged and then resuspended in this buffer containing 10 μM Sytox Green (Invitrogen) and 100 μg/ml RNaseA. Fluorescence distributions containing ~100 000 cells were recorded on a BD LSR II flow cytometer with a 488-nm laser excitation and a 525-nm emission filter, with signal acquisition triggered on the side-scatter parameter. All samples were acquired using identical voltage settings.

For microscopy, cells were sampled at the same time as those for flow cytometry in Figure 2D and were prepared with the same method except the final resuspension contained 1 μg/ml DAPI

instead of Sytox Green/RNase. Cells were mounted on agarose pads containing DAPI and incubated for 20 min at room temperature before DIC and fluorescence imaging.

Purification of Xer-6H and anti-Xer antibodies

The *S. solfataricus* Xer protein was overproduced as a C-terminally hexa-Histidine tagged protein in *E. coli*. The crude extract was incubated at 70°C for 20 min, the lysate was clarified by centrifugation, and Xer-6H was purified from the supernatant in batch by Ni-NTA chromatography, using standard methods with 2 × TBS as the buffer base. Heparin-sepharose chromatography was used as an additional step for Xer recombination reactions. Protein concentration was measured by absorbance at 280 nm, assuming $E_{280} = 24\,410\ M^{-1}\ cm^{-1}$. Antisera were raised against Xer-6H in rabbits. Antibodies were affinity purified from serum using Xer-6H immobilized on an NHS-activated agarose Hi-Trap column (GE Healthcare), and were eluted with 0.1 M glycine (pH 2.5) before neutralization and storage.

ChIP with microarray (ChIP-chip) and qPCR analysis

Mid-log phase *S. solfataricus* P2 cells were formaldehyde-fixed and total cell extracts were prepared in TBSTT buffer as described (Robinson *et al*, 2004). Extracts were sonicated to achieve a sheared DNA size range of ~0.5–2.0 kb, and then centrifuged for 10 min at 13 000 r.p.m. at 4°C. In all, 1.5 ml of the supernatant (containing ~1.5 mg total protein by Bradford assay) was then gently mixed at 4°C for ~18 h with 100 μl Dynabeads-Protein A (Invitrogen), which had been pre-loaded with 20 μg affinity-purified antibody and then washed twice with 1 ml TBSTT. Beads were then washed five times with 1 ml TBSTT, and then DNA was recovered as described (Robinson *et al*, 2004), without the back-extraction step. In all, 10 ng of the recovered DNA was labelled with Cyanine dyes, as described (Duggin *et al*, 2008a), as was 500 ng 'input' DNA purified from extract that had not been incubated with beads. Hybridization, including flip-dye replicates, with *S. solfataricus* microarrays (Isogen, de Meem, the Netherlands) was carried out as described (Duggin *et al*, 2008a), with the final scanning done at PMT voltages that gave no saturated spots. The intensity ratios of ChIP to input DNA for spots representing protein-encoding genes that passed quality control (Saeed *et al*, 2006) were then determined. Real-time quantitative PCR was carried out as described (Duggin *et al*, 2008a), with the dif1 and dif2 primer pairs, further below, and the following two control primer pairs:

oriC3-F:	CAGACATTTTCACTGATTTATTAGTTGAC
oriC3-R:	GGTGTTAGAATAGGCCTATCAAAGAG
lrs14-F:	GCAAGTAGAGAATATAAGAGTT
lrs14-R:	GAGAATAAGTCAGCACAATATT

Electrophoretic mobility-shift assays

PCR products were obtained using the following primer pairs and *S. solfataricus* P2 genomic DNA. PCR products were then digested with *Eco*RI and purified, prior to end labelling with Klenow.

dif1-R:	CCGGAATTCTTGAAAGTTACTTGTGATTCCACCT,
dif1-F:	CCGGAATTCGCGTTCAAGACTACATCTAATTCGT,
dif2-R:	CCGGAATTCTTGCGTAATACACGTAAGGAAAAC,
dif2-F:	CCGGAATTCAAACTTAGGTGGAATCACAAGTAAC,
dif3-R:	CCGGAATTCATAGGAAATAATCAGAATGGGGTA,
dif3-F:	CCGGAATTCAAAAGGCTATCTAAATTGTGTTTTCC,
dif4-R:	CCGGAATTCATGCCAAATAAAAATTAGGATG AGA,
dif4-F:	CCGGAATTCAGTTCCTAAAATCAACGATACAACG.

Double-stranded oligonucleotides corresponding to the dyad symmetric elements in the dif3 PCR amplicon were generated by annealing the following oligonucleotide pairs after radiolabelling with γ-^{32}P-ATP and polynucleotide kinase.

DYAD1U:	TTGTGTTTTCCTTACGTGTATTACGCAAGGAAGGTATT
DYAD1L:	AATACCTTCCTTGCGTAATACACGTAAGGAAAACACAA
DYAD2U:	TAACTGGAGGTTAACTTGTCAAGTTGACCTAACTCTTT
DYAD2L:	AAAGAGTTAGGTCAACTTGACAAGTTAACCTCCAGTTA

Purified Xer-6H and ^{32}P-labelled DNA fragments were mixed and then incubated for 1 h at room temperature at the concentrations indicated in Figure 4 in a buffer containing 20 mM Tris–Cl (pH 7.4), 50 mM NaCl, 1 mM EDTA, 50 μg/ml BSA, 50 μg/ml poly-dGC DNA and 10% (v/v) glycerol. Samples were loaded onto running polyacrylamide gels in 0.5 × TBE buffer. After electrophoresis, gels were fixed with a solution of 10% ethanol and 10% acetic acid (v/v), and then dried and exposed to a storage phosphor screen.

Xer recombination reactions in vitro

Intermolecular recombination reactions contained 200 ng of supercoiled plasmid and Xer-6H (16, 31 and 62.5 nM) in a volume of 20 μl. Intramolecular recombination reactions contained 400 ng of supercoiled plasmid and Xer-6H (62.5 nM) in a volume of 20 μl. The reaction buffer contained 20 mM Tris–HCl (pH 7.4), 50 mM KCl, 10 mM $MgCl_2$, 1 mM DTT, 5 mM spermine and 20% (v/v) glycerol. Reactions were incubated at 50°C for 2 h and then analysed by 0.8% (w/v) agarose gel electrophoresis in 1 × TAE followed by staining with SYBR green I (Sigma). Double-stranded oligonucleotides used to construct the plasmid substrates used in the recombination assays where generated by annealing the following oligonucleotides pairs:

dIII–dII U:	ACACTGTTCAGATAACTGGAGGTTAACTTGTCAAGTTG ACCTAACTCTTT
dIII–dII L:	AAAGAGTTAGGTCAACTTGACAAGTTAACCTCCAGTT ATCTGAACAGTGT
dII mutA U:	ACACTGTTCAGATAACTGGAGGTTAACTTGTCAGACCA GTTCGGTCTCCC
dII mutA L:	GGGAGACCGAACTGGTCTGACAAGTTAACCTCCAGTT ATCTGAACAGTGT
dII mutB U:	ACACTGTTCAGATAACTGGAGGTTAACTCACCAGACCA GTTCGGTCTCCC
dII mutB L:	GGGAGACCGAACTGGTCTGGTGAGTTAACCTCCAGTT ATCTGAACAGTGT
dIII mut U:	GTGTCACCTGAGCGGTCAAAGGTTAACTTGTCAAGTT GACCTAACTCTTT
dIII mut L:	AAAGAGTTAGGTCAACTTGACAAGTTAACCTTTGACC GCTCAGGTGACAC
dIII U:	TACACTGTTCAGATAACTGGAGGTTAACTTGTCAAGTT
dIII L:	AACTTGACAAGTTAACCTCCAGTTATCTGAACAGTGTA

Supplementary data

Supplementary data are available at *The EMBO Journal* Online (http://www.embojournal.org).

Acknowledgements

We thank Christian Lesterlin and Dave Sherratt for valuable discussions. This work was supported by the Medical Research Council and the Biotechnology and Biological Sciences Research Council, UK.

Author contributions: IGD, ND and SDB designed the experiments, performed the experiments and wrote the paper.

Conflict of interest

The authors declare that they have no conflict of interest.

References

Albers SV, Driessen AJ (2008) Conditions for gene disruption by homologous recombination of exogenous DNA into the *Sulfolobus solfataricus* genome. *Archaea* **2:** 145–149

Aussel L, Barre FX, Aroyo M, Stasiak A, Stasiak AZ, Sherratt D (2002) FtsK is a DNA motor protein that activates chromosome dimer resolution by switching the catalytic state of the XerC and XerD recombinases. *Cell* **108:** 195–205

Bigot S, Saleh OA, Lesterlin C, Pages C, El Karoui M, Dennis C, Grigoriev M, Allemand JF, Barre FX, Cornet F (2005) KOPS: DNA motifs that control *E coli* chromosome segregation by orienting the FtsK translocase. *EMBO J* **24:** 3770–3780

Bigot S, Sivanathan V, Possoz C, Barre FX, Cornet F (2007) FtsK, a literate chromosome segregation machine. *Mol Microbiol* **64:** 1434–1441

Brewer BJ, Fangman WL (1988) A replication fork barrier at the 3′ end of yeast ribosomal-RNA genes. *Cell* **55:** 637–643

Calzada A, Hodgson B, Kanemaki M, Bueno A, Labib K (2005) Molecular anatomy and regulation of a stable replisome at a paused eukaryotic DNA replication fork. *Genes Dev* **19:** 1905–1919

Carnoy C, Roten CA (2009) The *dif*/Xer recombination systems in proteobacteria. *PLoS One* **4:** e6531

Duggin IG, Bell SD (2009) Termination structures in the *Escherichia coli* chromosome replication fork trap. *J Mol Biol* **387:** 532–539

Duggin IG, McCallum SA, Bell SD (2008a) Chromosome replication dynamics in the archaeon *Sulfolobus acidocaldarius*. *Proc Natl Acad Sci USA* **105:** 16737–16742

Duggin IG, Wake RG, Bell SD, Hill TM (2008b) The replication fork trap and termination of chromosome replication. *Mol Microbiol* **70:** 1323–1333

Friedman KL, Brewer BJ (1995) Analysis of replication intermediates by two-dimensional agarose gel electrophoresis. *Meth Enzymol* **262:** 613–627

Hendricks EC, Szerlong H, Hill T, Kuempel P (2000) Cell division, guillotining of dimer chromosomes and SOS induction in resolution mutants (*dif*, *xerC* and *xerD*) of *Escherichia coli*. *Mol Microbiol* **36:** 973–981

Kuempel PL, Henson JM, Dircks L, Tecklenburg M, Lim DF (1991) *dif*, a recA-independent recombination site in the terminus region of the chromosome of *Escherichia coli*. *New Biol* **3:** 799–811

Lemon KP, Kurtser I, Grossman AD (2001) Effects of replication termination mutants on chromosome partitioning in *Bacillus subtilis*. *Proc Natl Acad Sci USA* **98:** 212–217

Lesterlin C, Pages C, Dubarry N, Dasgupta S, Cornet F (2008) Asymmetry of chromosome replichores renders the DNA translocase activity of FtsK essential for cell division and cell shape maintenance in *Escherichia coli*. *PLOS Genet* **4:** e1000288

Lundgren M, Andersson A, Chen LM, Nilsson P, Bernander R (2004) Three replication origins in *Sulfolobus* species: Synchronous initiation of chromosome replication and asynchronous termination. *Proc Natl Acad Sci USA* **101:** 7046–7051

Myllykallio H, Lopez P, Lopez-Garcia P, Heilig R, Saurin W, Zivanovic Y, Philippe H, Forterre P (2000) Bacterial mode of replication with eukaryotic-like machinery in a hyperthermophilic archaeon. *Science* **288:** 2212–2215

Nolivos S, Pages C, Rousseau P, Le Bourgeois P, Cornet F (2010) Are two better than one? Analysis of an FtsK/Xer recombination system that uses a single recombinase. *Nucleic Acids Res* **38:** 6477–6489

Pérals K, Cornet F, Merlet Y, Delon L, Louarn JM (2000) Functional polarization of the *Escherichia coli* chromosome terminus: the *dif* site acts in chromosome dimer resolution only when located between long stretches of opposite polarity. *Mol Microbiol* **36:** 33–43

Poplawski A, Bernander R (1997) Nucleoid structure and distribution in thermophilic Archaea. *J Bacteriol* **179:** 7625–7630

Robinson NP, Blood KA, McCallum SA, Edwards PAW, Bell SD (2007) Sister chromatid junctions in the hyperthermophilic archaeon *Sulfolobus solfataricus*. *EMBO J* **26:** 816–824

Robinson NP, Dionne I, Lundgren M, Marsh VL, Bernander R, Bell SD (2004) Identification of two origins of replication in the single chromosome of the archaeon *Sulfolobus solfataricus*. *Cell* **116:** 25–38

Saeed AI, Bhagabati NK, Braisted JC, Liang W, Sharov V, Howe EA, Li J, Thiagarajan M, White JA, Quackenbush J (2006) TM4 microarray software suite. *Meth Enzymol* **411:** 134–193

Samson RY, Obita T, Freund SM, Williams RL, Bell SD (2008) A role for the ESCRT system in cell division in archaea. *Science* **322:** 1710–1713

She Q, Singh RK, Confalonieri F, Zivanovic Y, Allard G, Awayez MJ, Chan-Weiher CCY, Clausen IG, Curtis BA, De Moors A, Erauso G, Fletcher C, Gordon PM, Heikamp-de Jong I, Jeffries AC, Kozera CJ, Medina N, Peng X, Thi-Ngoc HP, Redder P *et al* (2001) The complete genome of the crenarchaeon *Sulfolobus solfataricus* P2. *Proc Natl Acad Sci USA* **98:** 7835–7840

Sherratt DJ (2003) Bacterial chromosome dynamics. *Science* **301:** 780–785

Sivanathan V, Emerson JE, Pages C, Cornet F, Sherratt DJ, Arciszewska LK (2009) KOPS-guided DNA translocation by FtsK safeguards *Escherichia coli* chromosome segregation. *Mol Microbiol* **71:** 1031–1042

Toro E, Shapiro L (2010) Bacterial chromosome organisation and dynamics. *Cold Spring Harb Perspect Biol* **2:** a000349

Szabó Z, Sani M, Groeneveld M, Zolghadr B, Schelert J, Albers SV, Blum P, Boekema EJ, Driessen AJ (2007) Flagellar motility and structure in the hyperthermophilic archaeon *Sulfolobus solfataricus*. *J Bacteriol* **189:** 4305–4309

Val ME, Kennedy SP, El Karoui M, Bonné L, Chevalier F, Barre FX (2008) FtsK-dependent dimer resolution on multiple chromosomes in the pathogen *Vibrio cholerae*. *PLoS Genet* **4:** e1000201

Zhang R, Zhang CT (2005) Identification of replication origins in archaeal genomes based on the Z-curve method. *Archaea* **5:** 335–346